Studies of Heavy Pear-shaped Nuclei

P A Butler[1*]

[1]Department of Physics, University of Liverpool, Liverpool L69 7ZE, UK

Abstract. For certain combinations of protons and neutrons it is expected that the shape of atomic nuclei can undergo octupole deformation, which would give rise to reflection asymmetry or a "pear shape". Here it is described how recent experiments carried out at CERN using REX-ISOLDE and HIE-ISOLDE and the Miniball gamma-ray spectrometer have provided evidence that several radium and radon isotopes have either stable pear shapes or are octupole vibrational in nature. It will be shown that the data on transition moments present some challenges for theory. The relevance of these measurements for atomic EDM searches, and the future prospects for this field, will also be discussed.

1. Introduction

It is well established by the observation of rotational bands that atomic nuclei can assume quadrupole deformation with axial and reflection symmetry, usually with the shape of a rugby ball. The distortion arises from long-range correlations between valence nucleons which becomes favourable when the proton and/or neutron shells are partially filled. For certain values of proton and neutron number it is expected that additional correlations will cause the nucleus to also assume an octupole shape ('pear-shape') where it loses reflection symmetry in the intrinsic frame [1]. The observation of low-lying quantum states in many nuclei with even Z, N having total angular momentum and parity of $I^{\pi} = 3^{-}$ is indicative of their undergoing octupole vibrations about a reflection-symmetric shape. Further evidence is provided by the sizeable value of the E3 moment for the transition to the ground state, indicating collective behaviour of the nucleons. However, the number of observed cases where the correlations are strong enough to induce a static pear-shape is much smaller. Strong evidence for this type of deformation comes from the observation of a particular behaviour of the energy levels for the rotating quantum system and from an enhancement in the E3 moment [2]. Prior to the present work experimental signatures have been observed for only two cases, ^{224}Ra [3] and ^{226}Ra [4]. In order to explore the extent of this phenomenon in this mass region the HIE-ISOLDE facility at CERN was employed to provide accelerated radioactive isotopes of radon and radium. In these experiments the level schemes of the previously unknown ^{224,226}Rn were determined and E1, E2 and E3 matrix elements in ^{222}Rn, ^{222}Ra and ^{228}Ra measured.

2. Results

2.1 Measurement of the level schemes of heavy radon isotopes

In the experiments described here [5,6], ^{224}Rn (Z = 86, N = 138) and ^{226}Rn (Z = 86, N = 140) ions were produced by spallation in a thick thorium carbide target bombarded by ~10^{13} protons s^{-1} at 1.4 GeV from the CERN PS Booster. The reaction products diffused and effused from the heated target via a cooled transfer line towards an enhanced plasma ion source, which was used to singly ionize (q = 1+) the Rn isotopes. The ions were accumulated and cooled in a Penning trap, REX-TRAP and delivered as a bunch to an electron-beam ion source, REX-EBIS at 500 ms intervals. Here, the charge-state of the ions was increased by charge breeding up to 51^{+}. The ions were accelerated in HIE-ISOLDE to an energy of 5.08 MeV/nucleon and bombarded secondary targets of 2.1 mg/cm^2 ^{120}Sn. In order to verify the identification technique, ^{222}Rn, was also accelerated to 4.23 MeV/u. The beam intensities were 8.10^6 ions/s for ^{222}Rn, 2.10^6 ions/s for ^{224}Rn and 10^5 ions/s for ^{226}Rn. The γ-rays emitted following the excitation of the target and projectile nuclei were detected in Miniball [7], an array of 24 high-purity germanium detectors, each with six-fold segmentation

* Corresponding author: peter.butler@liverpool.ac.uk

and arranged in eight triple-clusters. The scattered projectiles and target recoils were detected in a highly segmented silicon detector [8].

Prior to the present work, nothing was known about the energies and spins of excited states in ^{224,226}Rn, while de-exciting γ -rays from states in ^{222}Rn had been observed [9] up to $I^{\pi} = 13^{-}$. The chosen bombarding energies for ^{224,226}Rn were about 3% below the nominal Coulomb barrier energy at which the beam and target nuclei come close enough in head-on collisions for nuclear forces to significantly influence the reaction mechanism. For such close collisions the population of high-spin states will be enhanced, allowing the rotational behaviour of the nucleus to be elucidated. This is the method has been coined "unsafe Coulomb excitation" [10] as the interactions between the high-Z reaction partners is predominantly electromagnetic. It is not possible to precisely determine electromagnetic matrix elements because of the small nuclear contribution. The most intense excited states expected to be observed belong to the positive-parity rotational band, built upon the ground state. These states are connected by fast E2 transitions. In nuclei that are unstable to pear-shaped distortion, the other favoured excitation paths are to members of the octupole band, negative-parity states connected to the ground-state band by strong E3 transitions. These will decay to states in the ground-state band by fast E1 transitions. In order to determine which states are connected by these transitions, pairs of coincident γ-rays were examined. In this analysis, the energy spectrum of γ-rays coincident with one particular transition is generated by requiring that the energy of this 'gating' transition lies in a specific range. Typical spectra obtained this way are shown in figure 1. Each spectrum corresponds to a particular gating transition, background subtracted, so that the peaks observed in the spectrum arise from γ-ray transitions in coincidence with that transition.

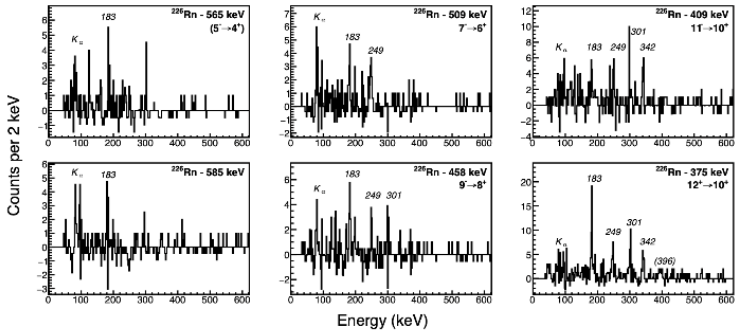

Figure 1. Coincidence γ-ray spectra. Representative background-subtracted γ-ray spectra for ^{226}Rn, in time-coincidence with different gating transitions. Here the observed peaks are labelled by the energy (in keV) of the transition. The gating transition is labelled by the proposed spin and parity of the initial and final states. See [5,6].

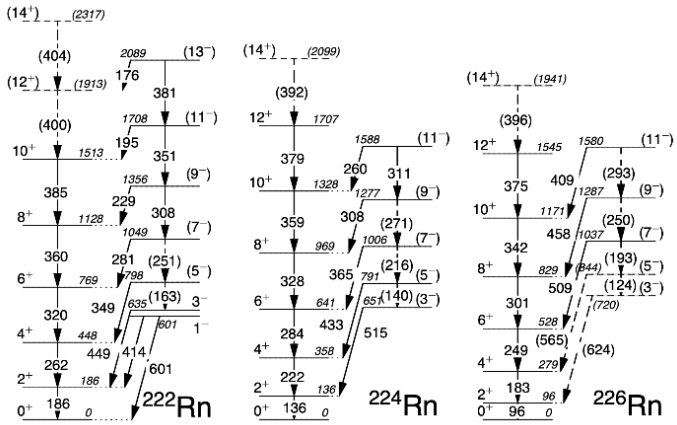

Figure 2. Rn Level schemes. These partial level-schemes for ^{222,224,226}Rn show the excited states of interest. Arrows indicate γ-ray transitions. All energies are in keV. Firm placements of transitions in the scheme are from previous work [9] or have been made using γ - γ coincidence relations; otherwise in brackets. See [5,6].

The level schemes for ^{224,226}Rn constructed from the coincidence spectra, together with the known [9] scheme for ^{222}Rn, are shown in figure 2. For ^{226}Rn the energy of the strongly-converted $2^+ \rightarrow 0^+$ transition overlaps with those of the K_β X-rays, but its value can be determined assuming that the relative intensity of K_β, K_α X-rays is the same as for ^{222,224}Rn. The E2 transitions connecting the states within the octupole band are not observed because they cannot compete with faster, higher-energy E1 decays to the ground-state band. The only other plausible description for this band is that it has $K^\pi = 0^+ \text{or } 2^+$, implying that the $K^\pi = 0^-$ octupole band is not observed. This is unlikely as the bandhead would have to lie significantly lower in energy than has been observed in ^{222,224,226}Ra, and inter-band transitions from states with $I' > 4$ to states with I and I-2 in the ground-state band and in-band transitions to I'-2 would all be visible in the spectra. The spin and parity assignments for the positive-parity band that is strongly populated by Coulomb excitation can be regarded as firm, whereas the negative-parity state assignments are made in accord with the systematic behaviour of nuclei in this mass region.

2.2 Characterisation of octupole instability from rotational behaviour

The character of the octupole bands can be explored [9] by examining the difference in aligned angular momentum, $\Delta i_x = i_x^- - i_x^+$, at the same rotational frequency ω, as a function of ω. Here i_x is approximately I for K=0 bands and $\hbar\omega$ is approximately $(E_I - E_{I-2})/2$. For nuclei with permanent octupole deformation Δi_x is expected to approach zero, as observed for several isotopes of Ra, Th, and U [11], see figure 3. For octupole vibrational nuclei in which the negative-parity states arise from coupling an octupole phonon to the positive-parity states, it is expected that $\Delta i_x \sim 3\hbar$ as the phonon prefers to align with the rotational axis. This is the case for the isotopes ^{218,220,222,224,226}Rn at values of $\hbar\omega$ (< 0.2 MeV) where particle-hole excitations do not play a role, see figure 3. Thus, the lower boundary at Z> 86 as to where permanent octupole deformation occurs in nature has been clearly delineated.

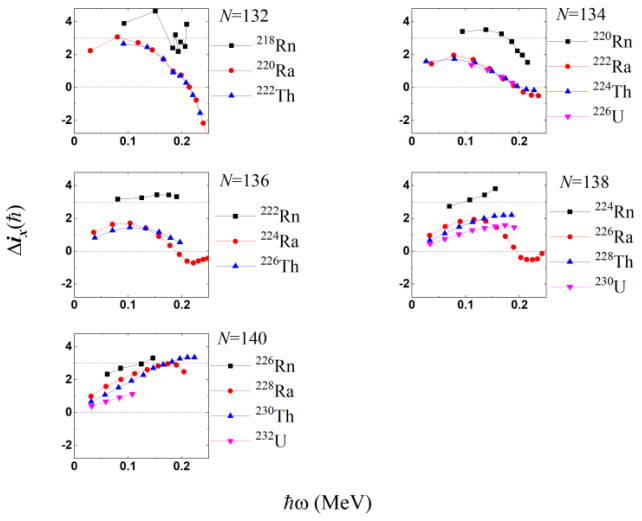

Figure 3. Systematic rotational behaviour of Rn, Ra, Th, U isotopes. The difference in aligned spin for negative- and positive-parity states in $^{218\text{-}226}$Rn, $^{220\text{-}228}$Ra, $^{222\text{-}230}$Th and ^{226,230,232}U as a function of rotational frequency. The dashed line at $\Delta i_x = 0$ is the expected value for static octupole deformation, the line at $\Delta i_x = 3\hbar$ corresponds to octupole vibration. Taken from [11].

2.3 Measurement of Eλ matrix elements in radon and radium isotopes

The radioactive isotopes ^{222}Ra (Z = 88, N = 134) and ^{228}Ra (Z = 88, N = 140) were produced by spallation in a thick uranium carbide primary target bombarded by $\approx 10^{13}$ protons/s at 1.4 GeV from the CERN PS Booster. The ions, extracted from a tungsten surface ion source were stripped to charge states of 51^+ and 53^+,

respectively, for ^{222}Ra and ^{228}Ra and accelerated in HIE-ISOLDE to an energy of 4.31 MeV/nucleon. The radioactive beams, with intensities between 5.10^4 and 2.10^5 ions/s bombarded secondary targets of ^{60}Ni and ^{120}Sn of thickness 2.1 mg/cm^2. Gamma rays emitted following the excitation of the target and projectile nuclei were detected in Miniball. The radioactive ^{222}Rn (Z = 86, N = 136) ions were produced as described in section 2.1 and accelerated in HIE-ISOLDE to 4.23 MeV/u. The accelerated ions then bombarded, with an intensity of 6.10^5 ions/s, the ^{60}Ni and ^{120}Sn targets as before. For these experiments the distance of closest approach $\geq R_1 + R_2 + 5$ fm, where R_1, R_2 are the beam, target nuclear radii, ensuring that the contribution from nuclear interactions is negligible [12].

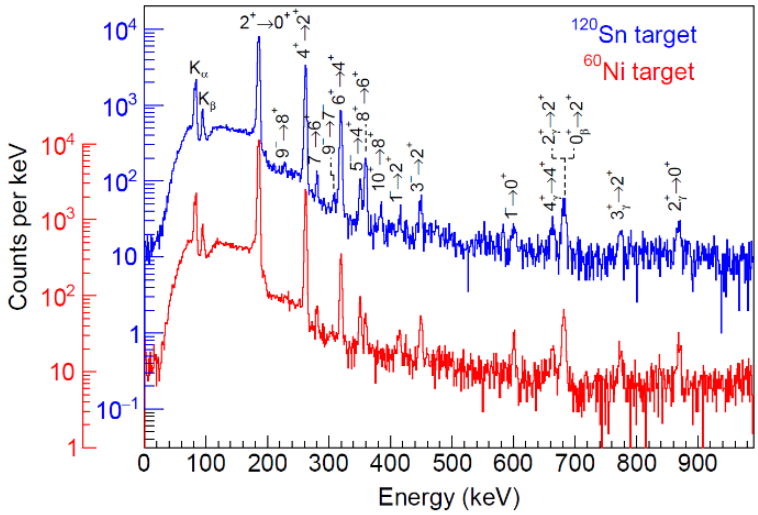

Figure 4. Spectra of γ rays emitted following Coulomb excitation of ^{222}Rn using a ^{120}Sn target (blue) and a ^{60}Ni target (red) observed in coincidence with recoiling target nuclei. The γ-ray energies were corrected for Doppler shift assuming they are emitted from the scattered projectile. Time-random coincidences between Miniball and the silicon detector have been subtracted. Taken from [12].

Representative γ-ray spectra obtained for ^{222}Rn from both the ^{120}Sn and ^{60}Ni targets are presented in figure 4. As the cross section for the Coulomb excitation of the projectile is strongly dependent on the atomic number of the target, the use of two targets with significantly different values of Z produce a different population of states in ^{222}Rn, ^{222}Ra and ^{228}Ra. In particular, the higher-Z target ^{120}Sn allows access to higher-spin states through multistep Coulomb excitation compared with ^{60}Ni. The spectra reveal a strong population of the positive-parity states of the ground-state band, which are populated via multiple $E2$ excitation. The population of negative-parity states of the octupole band, populated mostly by $E3$ excitation, is established via $E1$ decays to the positive parity states present in the spectra.

The matrix elements presented in this work [12,13] were obtained by using the Coulomb-excitation least-squares fitting code GOSIA [14]. GOSIA was employed to calculate excitation probabilities and subsequent γ-ray decay intensities of excited states for a given set of electromagnetic matrix elements. The calculated γ-ray intensities can be compared with the experimental yields and additional spectroscopic information that is available. In this work, known γ-ray branching ratios of low lying negative-parity states together with the measured γ-ray intensities were included in the calculations. A standard χ^2 function for both yields and branching ratios was constructed which was minimized by varying the values of the electromagnetic matrix elements between all relevant states, treated as free parameters.

In the case of ^{222}Rn, decays from two non-yrast bands, labelled as a β-band based on a $K^\pi=0^+$ state band-head, and a γ-band based on a $K^\pi = 2^+$ band-head were observed for the first time in this experiment [12] and their placement in the level scheme was determined through analysis of a γ-γ coincidence matrix collected with data from both targets. These bands were also observed in ^{228}Ra but were not visible for ^{222}Ra. For all three nuclei the excitation and decay of these low-lying collective bands were taken into account in the GOSIA fit; the decay of the β-band to the negative-parity states in particular influences the fitted values of the E3 matrix elements connecting the octupole and ground-state bands. In order to determine the systematic

sources of errors, a number of independent fits was obtained with different initial conditions. These included varying the target thickness, the beam energy, the distance between the target and the particle detector, the efficiency of the Miniball detectors, the *E*4 matrix elements, and the signs of the *E*2 couplings to the higher-lying collective bands.

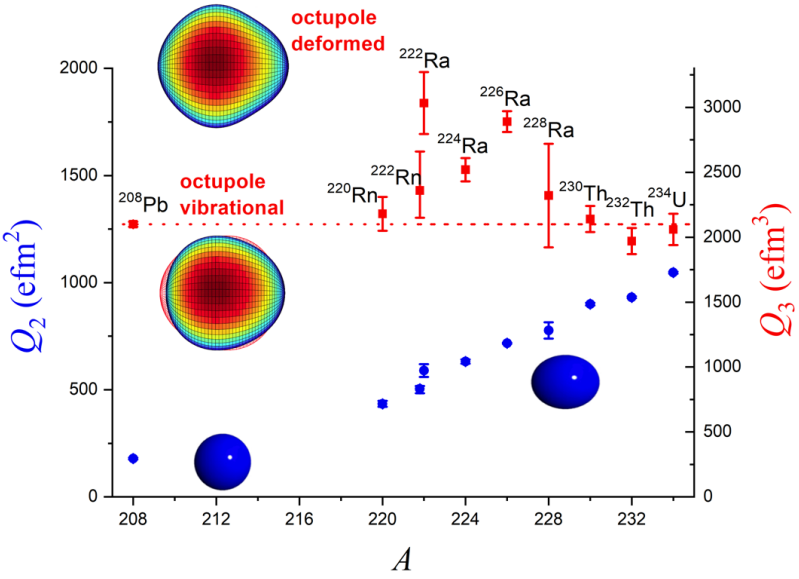

Figure 5. The systematics of measured E2 and E3 intrinsic moments Q_λ for $0^+ \rightarrow 2^+$ and $0^+ \rightarrow 3^-$ transitions, respectively, in the heavy mass region ($A \geq 208$). For the source of the data shown here, see fig. 4 in [11], and [12].

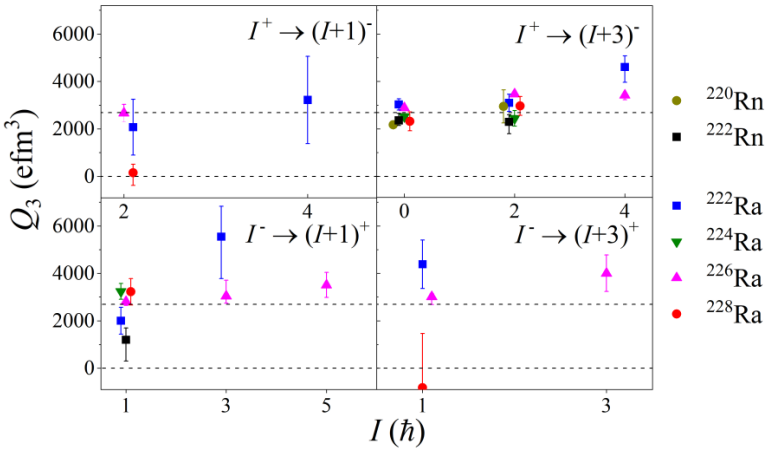

Figure 6. Values of the intrinsic octupole moments, Q_3, for various transitions in Rn and Ra isotopes. Here the values of Q_3 are shown separately for transitions connecting $I^+ \rightarrow (I+1)^-$, $I^+ \rightarrow (I+3)^-$, $I^- \rightarrow (I+1)^+$ and $I^- \rightarrow (I+3)^+$. The upper dashed line is the average value of $Q_3(0^+ \rightarrow 3^-)$ for $^{222\text{-}228}$Ra. The data are taken from [3], [4], [12], [13].

The measured quadrupole moment Q_2 and the octupole moment Q_3, for nuclei in the Z ~88, N ~134 mass region, are compared to those measured for adjacent heavy nuclei in figure 5. In this figure the intrinsic moments Q_λ are derived from the transition matrix elements $\langle I_i||M(E\lambda)||I_f\rangle$ corresponding to the $0^+ \rightarrow 2^+$ (E2) and $0^+ \rightarrow 3^-$ (E3) transitions, assuming the validity of the rotational model. It is striking that while the value of Q_2 increases by a factor of 6 between ^{208}Pb and ^{234}U, the value of Q_3 changes by only 50% in the entire mass

region. Nevertheless, the larger Q_3 values for ^{222}Ra, ^{224}Ra and ^{226}Ra indicate an enhancement in octupole collectivity that is consistent with an onset of octupole deformation in this mass region.

The values of the intrinsic electric octupole moment Q_3 for transitions in ^{220,222}Rn, ^{222,224,226,228}Ra are shown in Fig. 6. In the figure, the values of Q_3 are shown separately for transitions $I^+ \rightarrow (I+1)^-$, $I^+ \rightarrow (I+3)^-$, $I^- \rightarrow (I+1)^+$ and $I^- \rightarrow (I+3)^+$. It is observed that the values of Q_3 for all transitions in ^{222,224,226}Ra are approximately constant, consistent with the picture of a rotating pear shape. In contrast, the values of Q_3 corresponding to the $2^+ \rightarrow 3^-$ and $1^- \rightarrow 4^+$ transitions in ^{228}Ra do not show the same behaviour. There are insufficient data to make conclusions about the behaviour of the radon isotopes.

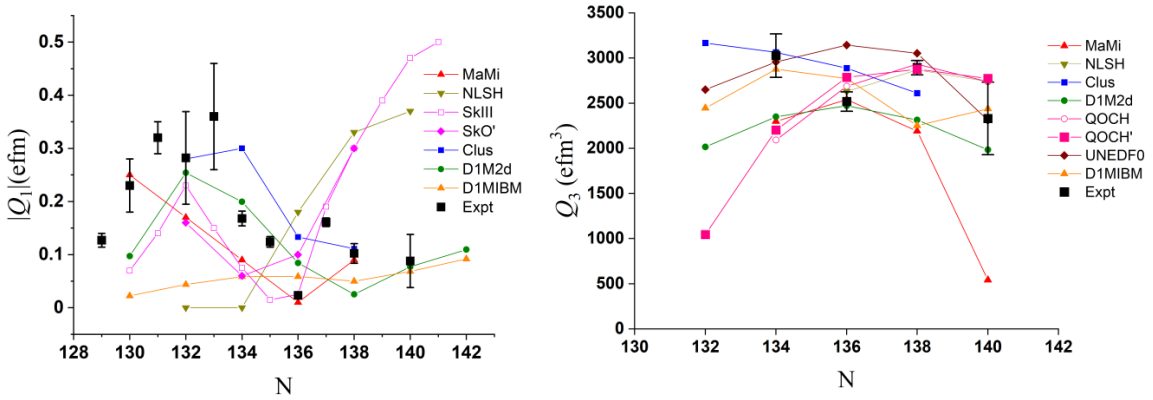

Figure 7. Measured values (Expt) of intrinsic octupole moments, Q_1 for $0^+ \rightarrow 1^-$ (left), and Q_3 for $0^+ \rightarrow 3^-$ (right) transitions as a function of N for radium isotopes, compared with values calculated using various theoretical models. For details of the calculations see the text.

The experimental values of intrinsic octupole moments Q_1 and Q_3 for radium isotopes, corresponding to the $0^+ \rightarrow 1^-$ (E1) and $0^+ \rightarrow 3^-$ transitions, are compared with various theoretical calculations in figure 7. The latter are from macroscopic-microscope (MaMi) [15,16], relativistic mean field (NLSH) [17], cranked Skyrme-Hartree-Fock (SkIII) [18], Skyrme-Hartree-Fock (SkO') [19], cluster model (Clus) [20], Gogny Hartree-Fock-Bogoliubov (D1M2d) [21], quadrupole-octupole collective Hamiltonian based on the PC-PK1 relativistic density functional (QOCH, QOCH') [22,23], Skyrme Hartree-Fock-Bogoliubov (UNEDF0) [24] and Gogny Hartree-Fock-Bogoliubov + interacting boson model (D1MIBM) [25] calculations. It can be seen that a wide variation in the predicted values of Q_3 from the different theories is evident, although no particular model description can be favoured or discarded on the basis of the experimental data. For the behaviour of Q_1 with neutron number, only the microscopic theories are able to exhibit a minimum around N = 134-138; not all of these are able to reproduce the observed minimum for ^{224}Ra. In contrast, there is good agreement between the various calculations and the experimental values of Q_2 [2].

3. Pear shapes and electric-dipole moments

The fact that some nuclei can have pear shapes has influenced the choice of atoms having odd-A nuclei employed to search for permanent electric-dipole moments (EDMs). Any measurable moment will be amplified if the nucleus has octupole collectivity and further enhanced by static-octupole deformation. At present, experimental limits on EDMs, that would indicate charge-parity (CP) violation in fundamental processes where flavour is unchanged, have placed severe constraints on many extensions of the Standard Model. For certain isotopes octupole effects are expected to enhance, by a factor 100-1000, the nuclear Schiff moment (the electric-dipole distribution weighted by radius squared) that induces the atomic EDM [26-29], thus improving the sensitivity of the measurement. There are two factors that contribute to the greater electrical polarizability that causes the enhancement: (i) the odd-A nucleus assumes an octupole shape; (ii) an excited state lies close in energy to the ground state with the same angular momentum and intrinsic structure but opposite parity. Such parity doublets arise naturally if the deformation is static (permanent octupole deformation). Candidate atomic species with nuclei having strong octupole

correlations, such as ^{221}Rn, ^{225}Ra, ^{229}Pa, have been proposed for EDM searches [30,31]. The measurements described in the previous section conclude that the even–even nuclei $^{222-226}$Ra have octupole-deformed character, and their odd-mass neighbours ^{223,225}Ra, having parity doublets separated by ≈50 keV, should have large enhancement of their Schiff moments. Measurements of the *E*3 strength in odd-*A* nuclei have yet to be carried out, however. For the octupole-vibrational radon isotopes, it appears unlikely that odd-*A* nuclei such as ^{221,223,225}Rn will have low-lying parity doublets, Bands of opposite parity with differing single-particle configurations can lie close to each other fortuitously but in general those arising from coupling the odd nucleon to the ground state and octupole phonon will be well separated. The separation will be determined by the spacing of the bands in the even-even core, ~500 keV in the case of $^{222-226}$Rn, and any enhancement of the Schiff moment will be smaller in radon atoms than for radium atoms.

4. Summary and outlook

There is now a substantial body of evidence, from the behaviour of the energies of quantum states and the interconnecting electromagnetic matrix elements, particularly electric octupole matrix elements, that a few isotopes of radium have permanent octupole deformation, i.e., are pear shaped. This is important not just for testing nuclear theories but also for improving the sensitivity of atomic EDM searches that could reveal the violation of fundamental symmetries not accounted for by the standard model. The systematic behaviour of energy levels in certain isotopes of thorium and uranium nuclei suggests that these may also be pear shaped. Several calculations using Gogny Hartree-Fock-Bogoliubov (D1M) [32], quadrupole-octupole collective Hamiltonian based on the PC-PK1 relativistic density functional (QOCH'') [33] and Gogny Hartree-Fock-Bogoliubov + interacting boson model (D1MIBM') [34] predict very large values of *E*3 moments in thorium and uranium isotopes with $N \approx 136$-138 (see figure 8). Experiments to measure *E*3 transition probabilities in these heavier nuclei, and in odd-mass nuclei relevant to EDM searches, await advances in radioactive beam technology that should be realized in the next few years.

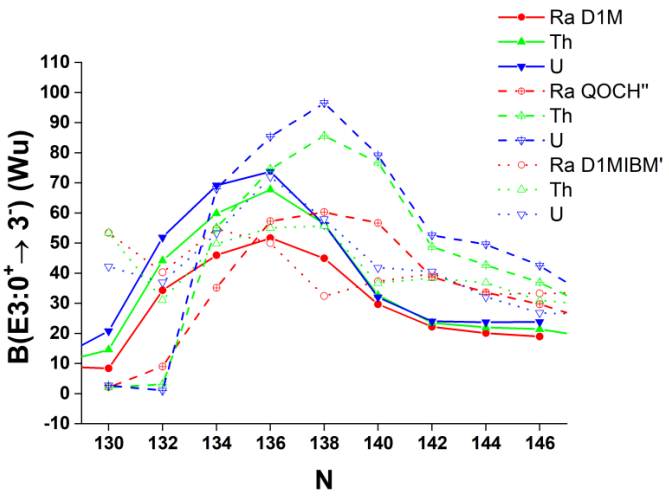

Figure 8. Theoretical values of $B(E3: 0^+ \rightarrow 3^-)$ transition strengths (in single particle units) versus N for various isotopes of Ra, Th and U. For details of the calculations see the text.

References

[1] Butler PA and Nazarewicz W 1996 *Rev. Mod. Phys.* **68** 349–421
[2] Butler PA 2016 *J. Phys. G: Nucl. Part. Phys.* **43** 073002
[3] Gaffney LP et al. 2013 *Nature* **497** 199-204
[4] Wollersheim HJ et al. 1993 *Nucl. Phys. A* **556** 261–280
[5] Butler PA et al. 2019 *Nat. Commun.* **10** 2473

[6] Butler PA et al. 2020 *Nat. Commun*. **11** 3560
[7] Warr N et al. 2013 *Eur.Phys. J. A* **49** 40
[8] Ostrowski A et al. 2002 *Nucl. Instrum. Methods A* **480** 448–455
[9] Cocks JFC et al. 1999 *Nucl. Phys. A* **645** 61–91
[10] Wiedenhöver I et al. 1999 *Phys. Rev. Lett.* **83** 2143-6
[11] Butler PA 2020 *Proc. R. Soc. London A* **476** 20200202
[12] Spagnoletti P et al. 2022 *Phys. Rev. C* **105** 024323
[13] Butler PA et al. 2020 *Phys. Rev. Lett.* **124** 042503
[14] Zielińska M et al. 2016 *Eur. Phys. J. A* **52** 99
[15] Nazarewicz W et al. 1984 *Nucl. Phys. A* **429** 269–295
[16] Butler PA and Nazarewicz W 1991 *Nucl. Phys. A* **533** 249–268
[17] Rutz K, Maruhn JA, Reinhard P-G and Greiner W. 1995 *Nucl. Phys. A* **590** 680–702
[18] Tsvetkov A, Kvasil J and Nazmitdinov RG 2002 *J. Phys. G: Nucl. Part. Phys.* **28** 2187–2206
[19] Engel J et al. 2003 *Phys. Rev. C* **68** 025501
[20] Shneidman TM et al. 2003 *Phys. Rev. C* **67** 014313
[21] Robledo LM and Butler PA 2013 *Phys. Rev.C* **88** 051302(R)
[22] Sun W et al. 2019 *Phys. Rev. C* **100** 044319
[23] Zhang W and Zhang SQ 2019 *Phys. Rev. C* **100** 054303
[24] Cao Y et al. 2020 *Phys. Rev. C* **102** 024311
[25] Nomura K et al. 2020 *Phys. Rev. C* **102** 064326
[26] Spevak V, Auerbach N and Flambaum VV 1997 *Phys. Rev. C* **56** 1357–1369
[27] Dobaczewski J and Engel J 2005 *Phys. Rev. Lett.* **94** 232502
[28] Ellis J, Lee J and Pilaftsis A 2011 *J. High Energy Phys.* **2011** 045
[29] Dobaczewski J et al. 2018 *Phys. Rev. Lett.* **121** 232501
[30] Auerbach N, Flambaum VV and Spevak V 1996 *Phys. Rev. Lett.* **76** 4316-4319
[31] Mohanmurthy P, Silwal U, Siwakoti DP and Winger JA 2020 *AIP Conf. Proc.* **2249** 030046
[32] Robledo LM and Bertsch GF 2011 *Phys. Rev. C* **84** 054302
[33] Xia SY et al. 2017 *Phys. Rev. C* **96** 054303
[34] Nomura K, Rodríguez-Guzmán R, Robledo LM and García-Ramos JE 2021 *Phys. Rev. C* **103** 044311

Acknowledgements

I am grateful to Niels Bidault, Eleftherios Fadakis, Karl Johnston, Miguel Lozano, Jose Alberto Rodriguez, Sebastian Rothe, Erwin Siesling, and Fredrick Wenander who assisted with the preparation of the radioactive beams, and Liam Gaffney, Pietro Spagnoletti, Joonas Konki, Marcus Scheck, John Smith, Kenzo Abrahams, Michael Bowry, Joakim Cederkäll, Timothy Chupp, Giacomo de Angelis, Hilde De Witte, Paul Garrett, Alina Goldkuhle, Corinna Henrich, Andres Illana, David Joss, James Keatings, Nicola Kelly, Michalina Komorowska, Thorsten Kröll, Bondili Nara Singh, David O'Donnell, Joonas Ojala, Robert Page, Line Pedersen, Christopher Raison, Peter Reiter, Dawid Rosiak, Timur Shneidman, Burkhard Siebeck, Michael Seidlitz, Jacqueline Sinclair, Marek Stryjczyk, Piet Van Duppen, Silvia Vinals, Ville Virtanen, Nigel Warr, Kasia Wrzosek-Lipska and Magda Zielinska who assisted with the data collection and analysis. The support of the ISOLDE Collaboration and technical teams is also acknowledged. I also thank Kosuke Nomura, Zhipan Li and Shuangquan Zhang for providing me with the results of their calculations. The work for these proceedings was supported by a grant from the Science and Technology Facilities Council ST/V001027/1.